

Motion in dynamical disorder - applications to 1/f noise and oscillator phase jitter

James P. Gleeson^a

^aApplied Mathematics, University College Cork, Ireland

ABSTRACT

Motion in Gaussian random space-time fields (“dynamical disorder”) is proposed as a model for certain dynamical systems where fluctuations play an important role. Analytical and numerical methods adapted from the study of passive scalar turbulence are applied to two examples: phase diffusion in noisy nonlinear oscillators and demonstrating the existence of 1/f phase noise in the mean field of Kuramoto’s coupled oscillators model.

Keywords: Diffusion, phase jitter, 1/f noise, coupled oscillators, Kuramoto model, turbulent transport.

1. INTRODUCTION

In this paper we study the scalar random processes $\theta(t)$ arising from the solution of equations of the form

$$\frac{d\theta}{dt} = F(\theta) + u(\theta, t), \quad (1)$$

with $F(\theta)$ denoting a deterministic function of θ , and $u(\theta, t)$ a Gaussian random field. The random field has mean zero

$$\langle u(\theta, t) \rangle = 0 \quad (2)$$

(angle brackets denote ensemble averages) and, being a Gaussian (i.e. multi-variate normal) field, its statistics are fully characterized by its correlation function

$$\langle u(\theta, t)u(\theta', t') \rangle. \quad (3)$$

The special case $F(\theta) \equiv 0$ proves instructive: then $\theta(t)$ is randomly advected by $u(\theta, t)$. This situation is analogous to the two-dimensional motion of a small buoy floating on the ocean surface, with position vector $\mathbf{x}(t)$ changing in response to the local velocity $\mathbf{u}(\mathbf{x}, t)$ of the sea waves¹:

$$\frac{d\mathbf{x}}{dt} = \mathbf{u}(\mathbf{x}, t), \quad (4)$$

and indeed many of our analytical and numerical methods for examining equation (1) are drawn from turbulent transport theory. Equation (4) may also be characterized as motion in “dynamical disorder” — the disorder being due to the θ -dependence of the stochastic function u , but ‘dynamical’ because u is also time-dependent. One limiting case of such dynamical disorder is the quenched disorder typical of percolation problems and flow through random media²; this arises when the time-dependence of $u(\theta, t)$ is very slow so that the randomness is essentially frozen on the timescales of interest. In a different limit, $u(\theta, t)$ may depend only very weakly on θ , so that it is effectively a stochastic process in time, and the equation (1) is then an example of the well-studied class of random differential equations with additive (white or coloured) noise.³

Motion in dynamical disorder has attracted recent research interest as a model for stock price dynamics⁴ and for diffusion in glassy systems.⁵ The analysis of equation (1) is non-trivial even for simple $F(\theta)$, as the dependence of the stochastic field u on θ makes the equation of motion inherently nonlinear. Results are obtainable using perturbation methods^{6,7} for the case of weak nonlinearity, as well as some special exactly-solvable cases.^{4,8}

Correspondence to j.gleeson@ucc.ie, telephone:+353 21 490 3410

Numerical methods for Monte-Carlo solutions of equation (1) have also been adapted from turbulent transport theory.⁹

In this paper we examine systems of physical and engineering interest that give rise to motion in dynamical disorder as in equation (1). More specifically, we concentrate here on the case where $F(\theta) \equiv U$, a constant, so that the deterministic motion is a constant drift with speed U . Moreover, a special type of dynamical disorder $u(\theta, t)$ arises naturally in our two examples: the so-called single-scale disorder which can be written⁸ as

$$u(\theta, t) = Y(t) \cos(\theta) - X(t) \sin(\theta). \quad (5)$$

Here $X(t)$ and $Y(t)$ are independent, stationary, zero-mean Gaussian coloured noise processes with variance κ^2 and correlation function R :

$$\langle X(t)X(t') \rangle = \langle Y(t)Y(t') \rangle = \kappa^2 R(t - t'). \quad (6)$$

We therefore have specialized equation (1) to

$$\frac{d\theta}{dt} = U + Y(t) \cos(\theta) - X(t) \sin(\theta). \quad (7)$$

In section 2 we demonstrate how equation (7) arises naturally in the study of oscillator phase jitter with coloured noise sources; section 3 examines the mean field phase dynamics in Kuramoto's^{10,11} model of coupled oscillators and shows that $1/f$ phase noise may be detected. A distinctive feature of the analysis in both examples is the importance of the spectral properties of the noise processes $X(t)$ and $Y(t)$ to the results. In particular it is shown that the spectrum $S(f)$ defined by

$$S(f) \equiv \frac{1}{2\pi} \int_{-\infty}^{\infty} R(\tau) e^{if\tau} d\tau \quad (8)$$

must have finite second moment, i.e., $\int_{-\infty}^{\infty} f^2 S(f) df < \infty$, in order to obtain certain interesting features. For example, the Ornstein-Uhlenbeck process which is often utilized as a model of coloured noise³ has infinite second spectral moment, so we also examine other coloured noise models to obtain our results.

2. PHASE DIFFUSION DUE TO COLOURED NOISE SOURCES

Noise sources in electronic oscillator circuits cause diffusion or jitter of the oscillator phase.¹² This causes timing jitter in clock circuits and broadening of the power spectrum peak, possibly leading to interference on nearby frequency bands in wireless communications applications. Accurately predicting this effect is therefore an important element of circuit design. In recent work, Demir and co-workers have proposed a general method for predicting phase diffusion in self-sustained oscillators in the presence of white¹³ and coloured¹⁴ noise sources. In this section we show that a simple two-dimensional oscillator model similar to that proposed by Coram¹⁵ leads to phase motion in dynamical disorder as in equation (7). Numerical simulations are used to compare the phase diffusion in this model to the predictions of Demir's general formula, and we highlight the need for higher-order corrections to that formula.

Consider a two-dimensional, noisy self-sustained oscillator described by the equations

$$\begin{aligned} \dot{x} &= \beta(1 - x^2 - y^2)x - \mu y + X(t) \\ \dot{y} &= \beta(1 - x^2 - y^2)y + \mu x + Y(t), \end{aligned} \quad (9)$$

which is simply the Cartesian form of the polar equations

$$\begin{aligned} \dot{r} &= \beta(1 - r^2)r + X(t) \cos \theta + Y(t) \sin \theta \\ \dot{\theta} &= \mu + \frac{Y(t)}{r} \cos \theta - \frac{X(t)}{r} \sin \theta. \end{aligned} \quad (10)$$

with $x = r \cos \theta$ and $y = r \sin \theta$, and dots denoting time derivatives. Note that such an oscillator is rather generic, arising from a Hopf bifurcation when the phase-amplitude coupling parameter is zero.¹⁶ The oscillator

frequency is μ , and the $X(t)$ and $Y(t)$ functions represent independent coloured noise sources in the original Cartesian variables. For simplicity we consider here the case when the oscillator amplitude r is confined close to the stable limit cycle at $r = 1$; in this case we can consider only the phase equation in the form

$$\dot{\theta} = \mu + Y(t) \cos \theta - X(t) \sin \theta. \quad (11)$$

The noise terms are Gaussian, of mean zero, and so are fully characterized by their correlation function (6). For definiteness, we choose the correlation function here to be

$$R(t) = \exp\left(-\frac{t^2}{2\tau^2}\right), \quad (12)$$

with τ being the correlation time.

Noting that equation (11) is similar to the single-scale dynamical disorder model (7), we are motivated to use numerical experiments to investigate the diffusion properties of (11), i.e. find the phase diffusion constant of the oscillator, and hence the phase jitter.¹⁴ Gaussian random functions may be constructed using a combination of a large number N of Fourier modes, as follows:

$$X(t) = \frac{1}{\sqrt{N}} \sum_{n=1}^N a_n \cos(\omega_n t) + b_n \sin(\omega_n t). \quad (13)$$

The amplitudes a_n and b_n are random numbers from a Gaussian distribution of mean zero and variance κ^2 . The ω_n are from a distribution shaped as the Fourier transform of $R(t)$ — for the correlation function we are using this means the ω_n are chosen from a zero-mean Gaussian distribution of variance $1/\tau$. The function constructed in this way is Gaussian in the limit $N \rightarrow \infty$ ^{4,17}; we use $N = 100$ in the experiments reported here.

In each realization, the independent noise functions are generated as above. The ordinary differential equation (11) is then solved numerically, using an initial condition of $\theta(0) = 0$, to find $\theta(t)$. The diffusion constant D is defined by the asymptotic relation

$$\text{var}(\theta) \sim D t \quad \text{as } t \rightarrow \infty, \quad (14)$$

where $\text{var}(\theta)$ is the variance of the distribution of phase values at time t :

$$\text{var}(\theta) \equiv \langle \theta^2(t) \rangle - \langle \theta(t) \rangle^2. \quad (15)$$

In the experiments, the variance is calculated at a large number of timesteps. A linear fit to the variance at large t gives the diffusion constant D as the slope of the fitted line.

The phase diffusion constant D is shown in Figure 1 for noise level $\kappa = 0.25$, and for a variety of values of the main oscillator frequency μ . The correlation time τ is normalized to unity in these calculations. An approximation, accurate to order κ^2 , to the phase diffusion constant may be calculated according to the method of Demir (equation (23) of his paper on coloured noise¹⁴):

$$\frac{d}{dt} (\text{var}(\theta)) = 2\kappa^2 \int_0^t \frac{1}{2} \left[e^{i\mu(t-s)} + e^{-i\mu(t-s)} \right] R(t-s) ds \quad (16)$$

and so in the limit of $t \rightarrow \infty$ we get

$$\begin{aligned} D &= 2\kappa^2 \int_0^\infty \cos(\mu s) e^{-s^2/2} ds \\ &= \sqrt{2\pi} \kappa^2 e^{-\frac{\mu^2}{2}}. \end{aligned} \quad (17)$$

This is plotted in Figure 1 with a dotted line, note it fits the numerical results well for moderate values of the oscillator frequency μ . However, at higher values of the frequency μ , the numerical results indicate that the diffusion constant is much larger than the (exponentially small) value predicted by Demir's formula. Indeed, we find an empirical fit (long-dashed line) which is proportional to $\kappa^4 \mu^{-2}$ — note that at large frequencies a

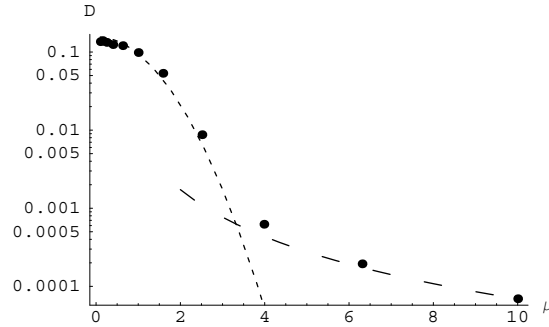


Figure 1. Phase diffusion D as a function of μ , with parameters $\kappa = 0.25$, $\tau = 1$. The dotted line shows the approximation (17); the long-dashed line is an empirical guess for the large- μ form in this case, $D \sim 0.007\mu^{-2}$.

power-law decay of D with μ is much slower than the exponential decay predicted in (17) and so can dominate, even at small noise intensities κ .

We have shown in this example that coloured noise in a simple oscillator causes phase diffusion which matches the formula of Demir¹⁴ at low oscillator frequencies, but seems to deviate at higher frequencies. Our further numerical experiments indicate that this result is generic — when the spectrum $S(f)$ of the coloured noise processes $X(t)$ and $Y(t)$ decays faster than f^{-2} at high frequencies a power-law scaling with μ of the phase diffusion emerges at high oscillator frequencies ($\mu \gg 1/\tau$). This effect is not captured by first-order (order κ^2) perturbation methods such as Demir’s, but the μ^{-2} scaling may be shown to arise as a general second-order (i.e. order κ^4) effect. We note that coloured noise processes of the type considered here can arise in many ways, for instance from filtered Ornstein-Uhlenbeck or white noise processes. It seems likely that this second-order effect will also be important in the high-frequency dynamics of more complex oscillators than the simple model (9) presented here. Current work focuses on testing for a μ^{-2} scaling range of the phase diffusion constant in general oscillators, and using higher-order perturbation theory to accurately predict the prefactor.

3. 1/F PHASE NOISE IN THE MEAN FIELD OF COUPLED OSCILLATORS

The term “1/f noise” is applied to random processes in time whose power spectrum scales with frequency f as $f^{-\alpha}$ for $\alpha \approx 1$ over a broad range of frequencies. Such processes are remarkably common in many applications in physics, engineering and applied sciences, see for example the website¹⁸ and review article.¹⁹ Electronic engineers are especially interested in 1/f noise and modelling thereof, as it is an important and poorly-understood component of phase noise in oscillator circuits.¹⁴ Many models of 1/f noise have been proposed, including an exactly-solvable model in discrete time,²⁰ but to our knowledge the oscillator ensemble phase noise examined here is the first exact solution for a continuous-time 1/f process.

Kuramoto’s¹⁰ model of coupled limit-cycle oscillators has been widely influential, with applications to synchronizing systems in a diversity of fields from biology,^{21,22} to Josephson junctions,²³ and semiconductor laser arrays.^{24,25} Strogatz¹¹ gives a pedagogical review of Kuramoto’s mean-field approach and its historical context; the theoretical predictions of synchronization have recently been confirmed experimentally using $N = 64$ chemical oscillators.²⁶ Synchronization of the ensemble is generally described in terms of the amplitude of the mean field of the oscillators; in this section we highlight the phase speed of the mean field, and show that it exhibits 1/f fluctuations.

In the Kuramoto model the phases $\theta_j(t)$ of N coupled oscillators are described by the equations

$$\dot{\theta}_j = \omega_j + \frac{\epsilon}{N} \sum_{k=1}^N \sin(\theta_k - \theta_j), \quad j = 1, \dots, N, \quad (18)$$

where the dot denotes time derivative. The native frequencies ω_j are chosen from a distribution $g(\omega)$ with mean Ω ; note that Ω may be set to zero without loss of generality by transforming to a rotating reference frame:

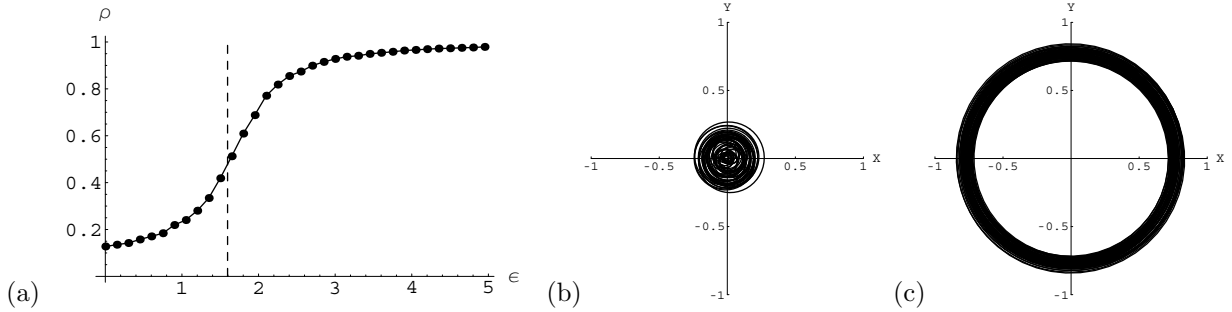


Figure 2. (a) Mean field amplitude $\langle \rho \rangle$ as a function of coupling strength ϵ , averaged over 100 realizations, for $N = 50$ oscillators. The critical coupling strength ϵ_c is shown with the dashed line; (b) An example of a mean-field trajectory in the (X, Y) plane, with $\epsilon = 0.3$ and $\Omega = 2\pi$; (c) As (b), but with $\epsilon = 1.9$.

$\theta_j \rightarrow \theta_j + \Omega t$, $\omega_j \rightarrow \omega_j - \Omega$. The coupling parameter ϵ determines the strength of interactions between individual oscillators. In the uncoupled ($\epsilon = 0$) case the oscillators are independent, but for sufficiently large ϵ the individual oscillators synchronize to a common frequency. The transition to synchronization is usually expressed in terms of the complex mean field (order parameter) of the oscillators, defined as

$$\rho e^{i\Theta} = X + iY = \frac{1}{N} \sum_{i=j}^N e^{i\theta_j}. \quad (19)$$

Note that the equation (18) for the phases may be rewritten in a similar form to equation (7) by using the mean field:

$$\dot{\theta}_j = \omega_j + \epsilon [Y(t) \cos \theta_j - X(t) \sin \theta_j]. \quad (20)$$

When the coupling is weak Daido²⁷ has shown that the mean field components $X(t)$ and $Y(t)$ are independent, zero-mean Gaussian process, and so the phase $\theta_j(t)$ moves in dynamical disorder as modelled by equation (7).

The amplitude ρ of the mean field is commonly used to indicate the onset of synchronization. Kuramoto¹⁰ showed that (in the $N \rightarrow \infty$ limit) the mean field amplitude ρ vanishes for $\epsilon < \epsilon_c$, where ϵ_c is the critical coupling strength given by

$$\epsilon_c = \frac{2}{\pi g(\Omega)}. \quad (21)$$

However, for $\epsilon > \epsilon_c$ the mean field amplitude grows as

$$\rho = \frac{4}{\epsilon_c^2} \sqrt{\frac{\epsilon - \epsilon_c}{-\pi g''(\Omega)}} \quad (22)$$

near the critical point, indicating a transition to synchronization (Fig. 2(a)). Trajectories in the (X, Y) plane are confined near the origin for $\epsilon < \epsilon_c$ (Fig. 2(b)), but trace out a limit cycle of radius ρ for $\epsilon > \epsilon_c$ (Fig. 2(c)). The angular speed of motion about the limit cycle is $\dot{\Theta} = \Omega$.

The effect of finite- N fluctuations upon these $N \rightarrow \infty$ theoretical results has been considered in a number of papers.^{27, 28} The mean field fluctuations scale as $N^{-\frac{1}{2}}$, and so the synchronization transition at $\epsilon = \epsilon_c$ is somewhat ‘smeared’ for finite N . Figure 2(a), for example, shows the average of the amplitude ρ over 100 realizations at various coupling strengths for $N = 50$ oscillators. The distribution of native frequencies is a Gaussian of mean Ω , with the variance normalized to unity:

$$g(\omega) = \frac{1}{\sqrt{2\pi}} e^{-\frac{(\omega - \Omega)^2}{2}}, \quad (23)$$

so the $N \rightarrow \infty$ critical point in equation (21) is $\epsilon_c \approx 1.60$. The effect of the finite- N fluctuations is clear; we note the similarity with the experimental results of Figure 2B of Kiss et al,²⁶ where $N = 64$ oscillators were used.

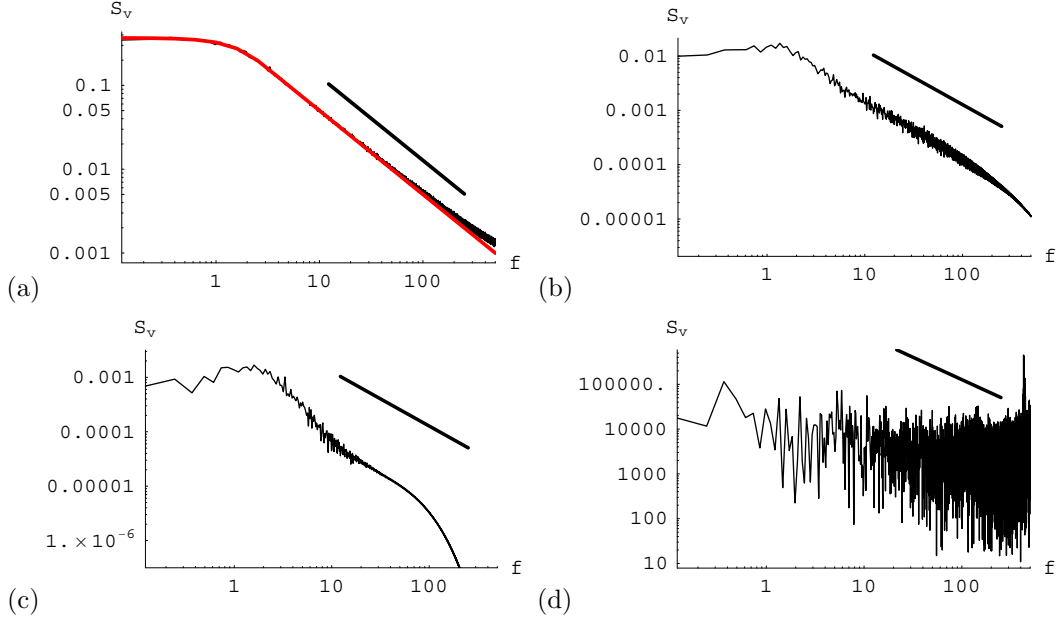


Figure 3. Average (over 1000 realizations) of the phase noise spectrum at various coupling strengths: (a) $\epsilon = 0$ for Gaussian $g(\omega)$; (b) $\epsilon = 1.9 (> \epsilon_c)$ for Gaussian $g(\omega)$; (c) $\epsilon = 2.3$ for Gaussian $g(\omega)$; (d) $\epsilon = 0$ for Lorentzian $g(\omega)$. Solid lines correspond to $1/f$ slopes in each case. The spectrum predicted from the exact result (33) is shown as a red curve in (a) and is almost indistinguishable from the numerical results.

The aim of this work is to highlight the effect of finite- N fluctuations upon the mean field phase speed $v(t) = \dot{\Theta}$. In particular we show that the stationary process $v(t)$ has a spectrum scaling as $1/f$ at high frequencies. In numerical experiments the time-dependent mean field phase speed is calculated as

$$\begin{aligned}
 v(t) = \dot{\Theta} &= \frac{d}{dt} \tan^{-1} \frac{Y}{X} \\
 &= \frac{X\dot{Y} - Y\dot{X}}{X^2 + Y^2}
 \end{aligned} \tag{24}$$

$$= \frac{\sum_{k=1}^N \sum_{j=1}^N \dot{\theta}_j \cos(\theta_k - \theta_j)}{\sum_{k=1}^N \sum_{j=1}^N \cos(\theta_k - \theta_j)}. \tag{25}$$

We calculate the spectrum of v by numerically solving the coupled equations (18) for $N = 50$ oscillators at various coupling parameters ϵ , taking the random initial phases $\theta_j(0)$ as uniformly distributed. We choose a Gaussian distribution $g(\omega)$ of native frequencies, setting the variance to unity by a suitable choice of timescale, and the mean to zero: $\Omega = 0$. After neglecting transients, in each realization a time series $v(t)$ of 2^{14} samples at intervals $\Delta t = 3.125 \times 10^{-3}$ is fast-Fourier transformed; the average spectrum over 1000 realizations is shown in Figure 3. A clear $1/f$ range in the spectrum is apparent for coupling strengths from sub-threshold levels up until the oscillators are all phase-locked at $\epsilon > \epsilon_c$. Moreover, the $1/f$ spectrum is present even in the $\epsilon = 0$ limit of uncoupled oscillators, Figure 3(a). This suggests that the $1/f$ spectrum of the mean phase speed is independent of the synchronization mechanism.

The uncoupled ($\epsilon = 0$) limit may be examined analytically. We note that since the oscillators are independent when $\epsilon = 0$, the mean field components $X = \frac{1}{N} \sum_{i=1}^N \cos(\omega_i t)$ and $Y = \frac{1}{N} \sum_{j=1}^N \sin(\omega_j t)$ are independent and (by the central limit theorem for large N) Gaussian. The autocorrelation function of X and Y defined by

$$\frac{\langle X(t)X(t+\tau) \rangle}{\langle X(t)^2 \rangle} = \frac{\langle Y(t)Y(t+\tau) \rangle}{\langle Y(t)^2 \rangle} = R(\tau) \tag{26}$$

is related directly to their power spectrum $S(f)$ by

$$S(f) \equiv \frac{1}{2\pi} \int_{-\infty}^{\infty} e^{if\tau} R(\tau) d\tau = g(f) \quad (27)$$

where g is the distribution function of the native frequencies of the oscillators. In a recent paper²⁹ we proved that when $X(t)$ and $Y(t)$ are independent zero-mean Gaussian processes with autocorrelation function $R(\tau)$ and finite second spectral moment, i.e., $\int_{-\infty}^{\infty} f^2 S(f) df < \infty$, then the correlation function $R_v(\tau)$ of the phase speed $v(t)$ defined in (24) is given by

$$R_v(\tau) \equiv \langle v(t)v(t+\tau) \rangle = \frac{1}{2R(\tau)^2} \{R(\tau)R''(\tau) - R'(\tau)^2\} \log [1 - R(\tau)^2]. \quad (28)$$

Provided that the correlation function $R(\tau)$ of X and Y is sufficiently smooth that $R''(0)$ exists, a small- τ expansion of the phase speed correlation $R_v(\tau)$ yields the asymptotic form

$$R_v(\tau) \sim -\frac{1}{2\tau_0^2} \log \left(\frac{\tau^2}{\tau_0^2} \right) \quad \text{as } \tau \rightarrow 0. \quad (29)$$

Here the timescale τ_0 is defined by the initial radius of curvature of $R(t)$:

$$\tau_0 \equiv [-R''(0)]^{-\frac{1}{2}}. \quad (30)$$

The phase speed spectrum $S_v(f)$ is the Fourier transform of $R_v(\tau)$, as in equation (27). The large frequency asymptotics of the spectrum follow from the small- τ expansion (29) of the correlation function using the method of steepest descents³⁰:

$$S_v(f) \sim \frac{1}{2\tau_0^2} \frac{1}{f} \quad \text{as } f \rightarrow \infty. \quad (31)$$

In fact for the Gaussian distribution $g(\omega)$ of native frequencies, it is easy to see that the correlation function $R(\tau)$ of the mean field components X and Y is

$$R(\tau) = e^{-\frac{\tau^2}{2}}, \quad (32)$$

and in this case equation (28) yields the phase speed correlation function

$$R_v(\tau) = -\frac{1}{2} \log [1 - e^{-\tau^2}]. \quad (33)$$

The predicted spectrum for the uncoupled case is determined by a numerical integration of the form (27) over the correlation function (33), and is almost indistinguishable from the numerical results, see Figure 3(a).

The condition on the finiteness of $R''(0)$, or equivalently of $\int_{-\infty}^{\infty} f^2 S(f) df$, imposed in the above analysis requires the distribution function $g(\omega)$ of native frequencies to have finite variance. While this is the case for the Gaussian $g(\omega)$ used above, the condition is violated if $g(\omega)$ is a Lorentzian (Cauchy) distribution. An exact solution for the $N \rightarrow \infty$ order parameter ρ was obtained by Kuramoto¹⁰ assuming a Lorentzian distribution of frequencies and so this distribution is popular in the coupled oscillators literature. However, Fig. 3(d) shows that $1/f$ phase noise spectra are not obtained when $g(\omega)$ has the Lorentzian form

$$\frac{1}{\pi(1 + \omega^2)}, \quad (34)$$

indicating that the finiteness of the variance of g is a necessary condition.

The $1/f$ tail of the spectra shown in Figure 3 has a lower-frequency cutoff at a ‘shoulder’ frequency of order one. Our nondimensionalization of time by the standard deviation ω_0 of the native frequencies implies that the dimensional shoulder frequency is approximately ω_0 . Thus a narrower distribution of native frequencies about the mean (lower ω_0) leads to a lower frequency shoulder in the $1/f$ spectrum.

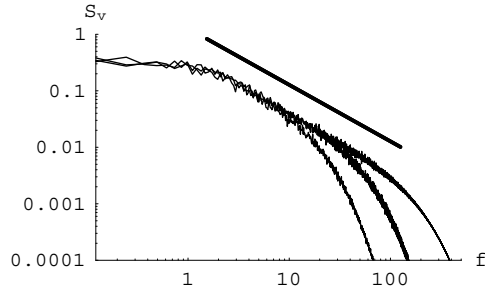


Figure 4. Spectrum of the phase speed $\dot{\theta}_N$ of the N th oscillator (for $N = 50$), with non-uniform couplings as in equation (35): $\epsilon_1 = \epsilon_2 = \dots = \epsilon_{N-1} = 0.3$, and for three different values of the strong coupling: $\epsilon_N = 10^5$ (top spectrum), $\epsilon_N = 10^4$, and $\epsilon_N = 10^3$ (bottom spectrum). Averages are taken over 100 realizations.

It is important to stress that the spectra shown in Figure 3 are those of the *mean field* phase speed, and their properties, including the $1/f$ scaling, are due to the collective effects of the N oscillators. By contrast, each individual oscillator, for instance the j th, has its own phase speed $\dot{\theta}_j$, which does not in general exhibit a $1/f$ spectrum. Indeed this is clear in the $\epsilon = 0$ limit, as the phase speed of the individual oscillator is the constant ω_j (giving a delta-spike spectrum), whereas the mean field phase speed $\dot{\Theta}$ has the rich spectrum of Figure 3(a). Nevertheless, it is interesting to consider situations in which $1/f$ scaling might be observed in the phase speed spectra of individual oscillators. One such scenario arises if each oscillator has its own coupling strength ϵ_j , so that equation (18) is modified to

$$\dot{\theta}_j = \omega_j + \epsilon_j \rho \sin(\Theta - \theta_j), \quad j = 1, \dots, N, \quad (35)$$

where the dependence on the mean field (19) has also been made explicit. Suppose now that the coupling strength of the first $N - 1$ oscillators is uniform and subthreshold ($\epsilon_j < \epsilon_c$ for $j = 1, \dots, N - 1$), but that the N th oscillator is very strongly coupled to the mean field, i.e., $\epsilon_N \gg \epsilon_c$. With the second term on the right-hand-side of equation (35) being dominant for $j = N$, the N th oscillator synchronizes with the mean field on a fast timescale, and so the spectrum of $\dot{\theta}_N$ is expected to display a $1/f$ range. Figure 4 shows the results of numerical simulations of $N = 50$ oscillators with $\epsilon_1 = \epsilon_2 = \dots = \epsilon_{N-1} = 0.3$, and for various large values of ϵ_N . When the N th oscillator is strongly coupled to the mean field, its phase speed develops a $1/f$ spectrum over a frequency range which grows with the coupling strength.

4. DISCUSSION

We have examined two examples from engineering applications where the single-scale motion in dynamical disorder, equation (7), arises naturally. The effect of fluctuations in such systems is quite distinct from those generated by additive noise.³

In section 2 we calculated the phase diffusion in a self-sustained oscillator due to coloured noise sources, and showed that the general method of Demir¹⁴ requires a correction for certain noise sources. Specifically, higher-order perturbation theory gives a $\kappa^4 \mu^{-2}$ correction to Demir's order $\kappa^2 S(\mu)$ formula, and the correction term can dominate at high frequencies μ when the spectrum $S(f)$ of the coloured noise decays faster than f^{-2} .

In section 3 the mean field phase speed $\dot{\Theta}$ of Kuramoto's coupled oscillators model is shown to have a $1/f$ spectrum, provided that the distribution $g(\omega)$ of native frequencies has finite variance. An analytical result is derived for the uncoupled $\epsilon = 0$ case, but numerical solutions indicate the persistence of the $1/f$ scaling somewhat above the synchronization threshold, see Figures 2(c) and 3(b) for instance.

The study of single-scale dynamical disorder, equation (5) has thus led to new and interesting applied results in two rather different examples. It is anticipated that the general case, equation (1), will require further mathematical advances, and lead to significant increases in the understanding of systems where fluctuations play an important role.

5. ACKNOWLEDGEMENTS

This work is supported by funding from Science Foundation Ireland Investigator Award 02/IN.1/IM062. The author gratefully acknowledges the motivational questions on $1/f$ noise originally posed by Colin Lyden of Analog Devices.

REFERENCES

1. A. M. Balk, *J. Fluid Mech.* **467**, 163 (2002).
2. J-P. Bouchard and A. Georges, *Phys. Reports*, **195**, 127 (1990).
3. F. Moss and P. V. E. McClintock ed. *Noise in nonlinear dynamical systems* (Cambridge University Press, Cambridge, 1979).
4. J. P. Gleeson, "Passive motion in dynamical disorder as a model for stock market prices," *Physica A*, to appear; see also J. P. Gleeson arxiv.org/cond-mat/0311646 (2003).
5. J. B. Witkoskie, S. Yang, and J. Cao, *Phys. Rev. E* **66**, 051111 (2002).
6. J. P. Gleeson, *Phys. Fluids*, **12**, 1472 (2000).
7. J. P. Gleeson and D. I. Pullin, *Phys. Fluids*, **15**, 3546 (2003).
8. J. P. Gleeson, *Phys. Rev. E*, **65**, 037103 (2002).
9. A. J. Majda and P. R. Kramer, *Phys. Rep.*, **314**, 237 (1999).
10. Y. Kuramoto, *Chemical oscillations, waves, and turbulence* (Springer, Berlin, 1984).
11. S. H. Strogatz, *Physica D*, **143**, 1 (2000).
12. F. X. Kaertner, *Int. J. Circuit Theory and Appl.*, **18**, 485 (1990).
13. A. Demir, A. Mehrotra, and J. Roychowdhury, *IEEE Trans. Circuits and Systems I*, **47**, 655 (2000).
14. A. Demir, *IEEE Trans. Circuits and Systems I*, **49**, 1782 (2002).
15. G. J. Coram, *IEEE Trans. Circuits and Systems I*, **48**, 896 (2001).
16. J. P. Gleeson and F. O'Doherty, "Non-Lorentzian spectral lineshapes near a Hopf bifurcation," preprint.
17. J. M. Ziman, *Models of disorder* (Cambridge University Press, Cambridge, 1979).
18. W. Li, *A bibliography on 1/f noise*, www.nslj-genetics.org/wli/1fnoise.
19. M. B. Weissman, *Rev. Mod. Phys.*, **60**, 537 (1988).
20. B. Kaulakys, *Phys. Lett. A*, **257**, 37 (1999).
21. F. C. Hoppensteadt and E. M. Izhikevich, *Weakly connected neural networks* (Springer, New York, 1997).
22. F. C. Hoppensteadt and E. M. Izhikevich, *Phys. Rev. Lett.*, **82**, 2983 (1999).
23. K. Wiesenfeld, P. Colet, and S. H. Strogatz, *Phys. Rev. Lett.*, **76**, 404 (1996).
24. S. Yu. Kourtchatov et al, *Phys. Rev. A*, **52**, 4089 (1995).
25. G. Kozyreff, A. G. Vladimiroc, and P. Mandel, *Phys. Rev. Lett.*, **85**, 3809 (2000).
26. I. Z. Kiss, Y. Zhai, and J. L. Hudson, *Science*, **296**, 1676 (2002).
27. H. Daido, *J. Stat. Phys.*, **60**, 753 (1990).
28. A. Pikovsky and S. Ruffo, *Phys. Rev. E.*, **59**, 1633 (1999).
29. J. P. Gleeson, "An exactly solvable model of continuous $1/f$ noise," submitted to *Phys. Rev. E.* (2004).
30. C. M. Bender and S. A. Orszag, *Advanced Mathematical Methods for Scientists and Engineers* (Springer, New York, 1999), pp. 280-282.